Chair of High-Power Converter Systems
TUM School of Engineering and Design
Technical University of Munich

Design of an External Current Measurement PCB for SiC Inverters

Kaan Ilhan

Technische Universität München

Chair of High-Power Converter Systems

06. August 2025

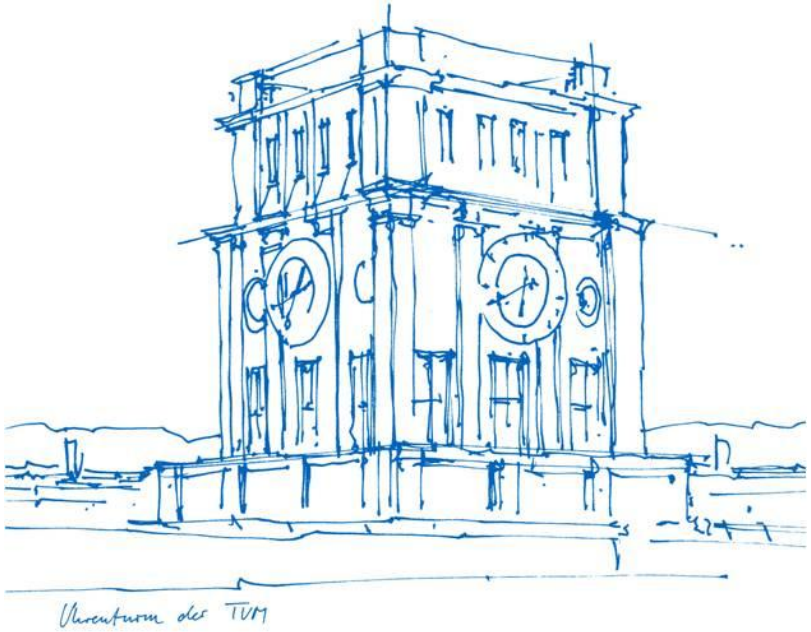

Agenda

1) Introduction & Motivation
2) Design of the Analog Current Measurement PCB
    a) Revision 1
    b) Revision 2
3) Sensor Technologies & Portfolio
4) Experimental Evaluation
    a) DC Accuracy & Linearity
    b) Noise & Frequency Behavior
    c) AC Impedance Characterization
5) Conclusion

Introduction & Motivation

- Accurate current sensing is critical in power electronics for control, protection, and efficiency.
- The rise of SiC and GaN semiconductors demands faster and more precise measurement.

- **Focus:** Accurate current sensing for high-current **three-phase SiC inverter** for motor drive.
  Suitability of current sensing in real-world

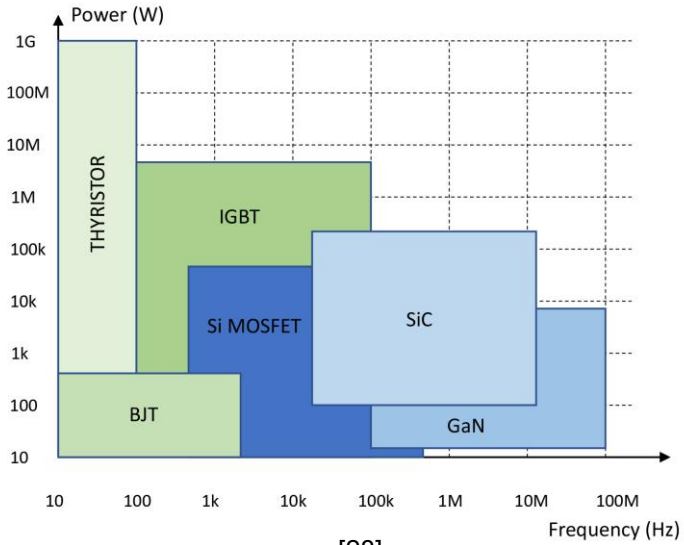

[28]

Current Sensing Approaches

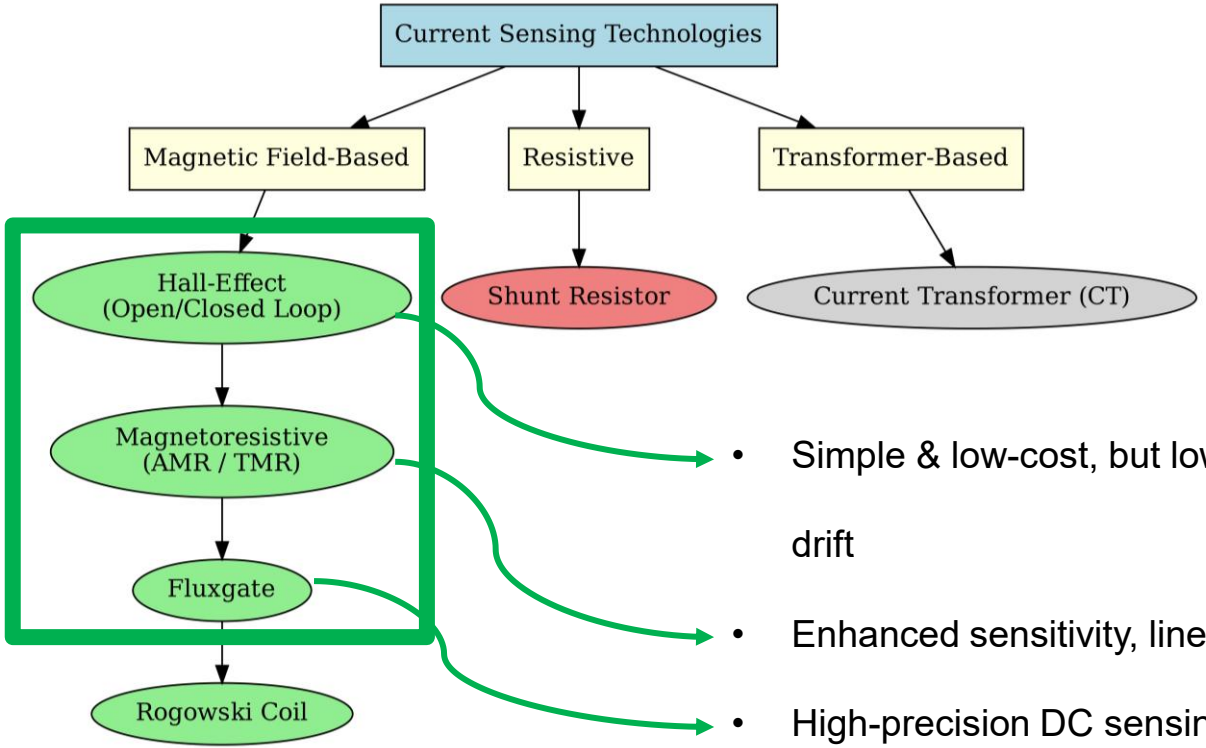

- Simple & low-cost, but lower accuracy and more drift
- Enhanced sensitivity, linearity, and lower noise
- High-precision DC sensing, but introduces modulation ripple

Sensor Topologies: Open-loop vs Closed-loop

Open-loop

[3]

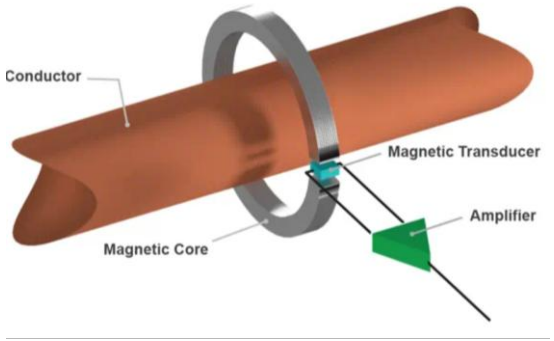

- Direct sensing
- Limited accuracy

Closed-loop (compensated)

[3]

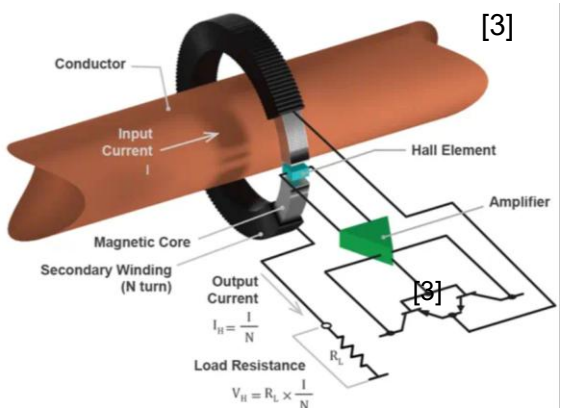

- Feedback coil
- Zero-flux

Current Measurement PCB Overview

- 4-layer PCB for analog current measurements with 4 channels
- Input Current: up to 57 A_{RMS} / 80 A_{peak}
- Supports sensors with THD-8 footprint (Sensitec CAS5000, LEM CASR etc.)
- Compatible with UltraZohm platform (RJ45 differential output)
- Thermal safe limit: 100 °C at 80 A continuous current (tested)
- V_{OCM}= 2.5 V
- Supply: 9–48 V input, step-down to 5.12 VCC+ (adjusted for full-scale swing)
- Phase-to-phase clearance/creepage: 2.5mm → maximum 500 V_{RMS}

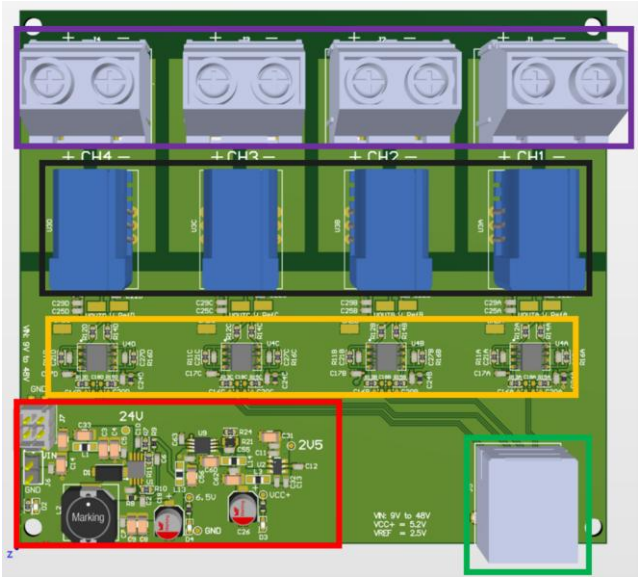

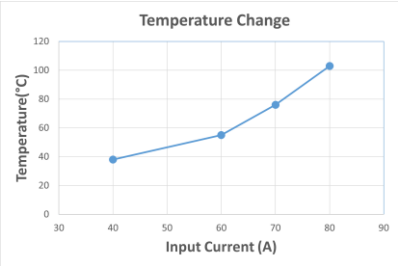

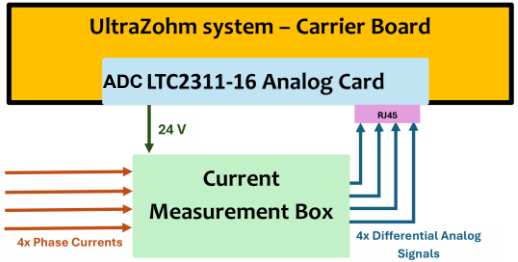

Current Measurement PCB/Box

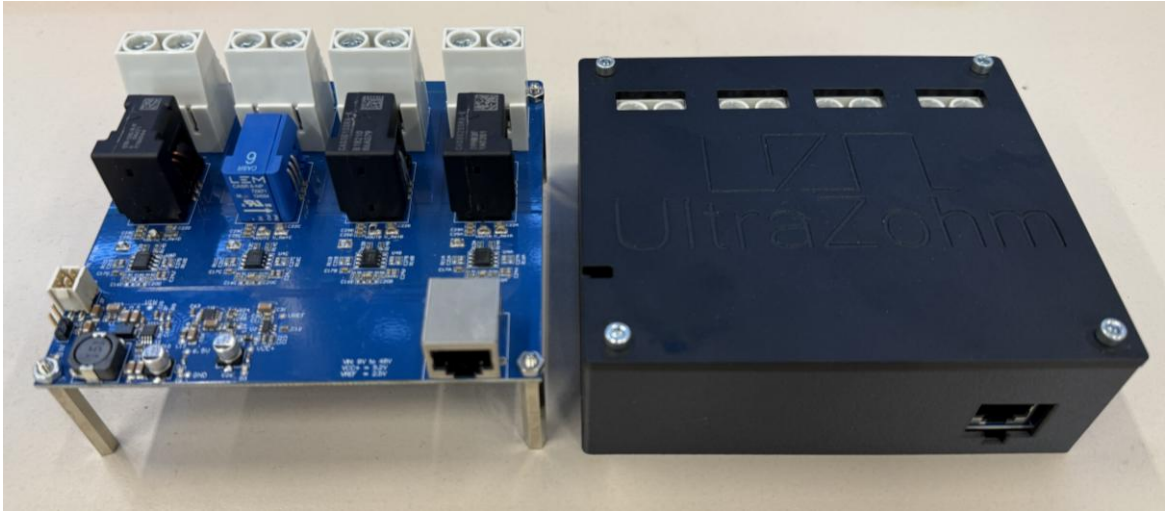

Experimental Evaluation 1

DC Measurement: Methodology

- DC sweep to measure differential output voltage ($V_{OUT+} - V_{OUT-}$)
- Measurement taken at RJ45 differential output (after op-amp stage)
- Linear fit applied to extract measured gain and offset

Sensors:

1) LEM CASR series: closed-loop Fluxgate
2) Sensitec/Sinomags 5000 series: closed-loop TMR

Sinomags STB-6 (TMR). $I_N = 6\ A_{RMS}$ (Range: ±20 A)

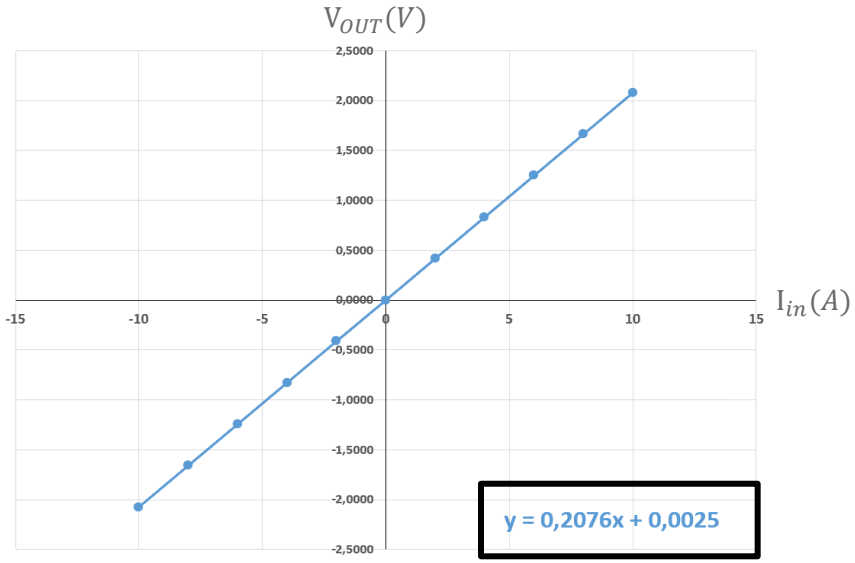

$$G_{\text{expected}} = \text{OpAmp Gain} \cdot \text{Sensor Sensitivity} = 2 \cdot 104.2\,\frac{\text{mV}}{\text{A}} = 208.4\,\frac{\text{mV}}{\text{A}}$$

$$G_{\text{measured}} = 207.6\,\frac{\text{mV}}{\text{A}} \quad \Rightarrow \quad \text{Relative Error} = 0.38\,\%$$

Experimental Evaluation 2

Time & Frequency Domain Observations: Methodology

- Sinusoidal current input: 1 A_{RMS} @ 500 Hz
- Single ended voltage probes for sensor outputs of closed-loop TMR (25 A) and Fluxgate sensors (25 A)
- If needed: Each output waveform is normalized by Gain → **normalized current-equivalent outputs**
- FFT analysis to identify: internal modulation tones (spikes), noise floor (broadband interference), whole spectral content
- Sensor bandwidth (300 kHz & 400 kHz) impacts:
    a. ripple suppression ability
    b. Signal fidelity
    c. Passing through more high-frequency noise

Experimental Evaluation 2

Time & Frequency Domain Observations

- **Closed-loop TMR (25 A)**: Slightly elevated noise floor. But overall flatter frequency spectrum with no internal modulation spikes.

  → smoother and less noisy time-domain output waveform

- **Closed-loop Fluxgate (25 A)**: higher ripple due to dominant internal excitation peak at ~435 kHz, as documented in datasheet

- **Closed-loop TMR (25 A)**: using Micsig optical isolated differential probes connected at the ethernet output, with differential output filter ($f_{cut-off} = 273\ kHz$)

Frequency Domain

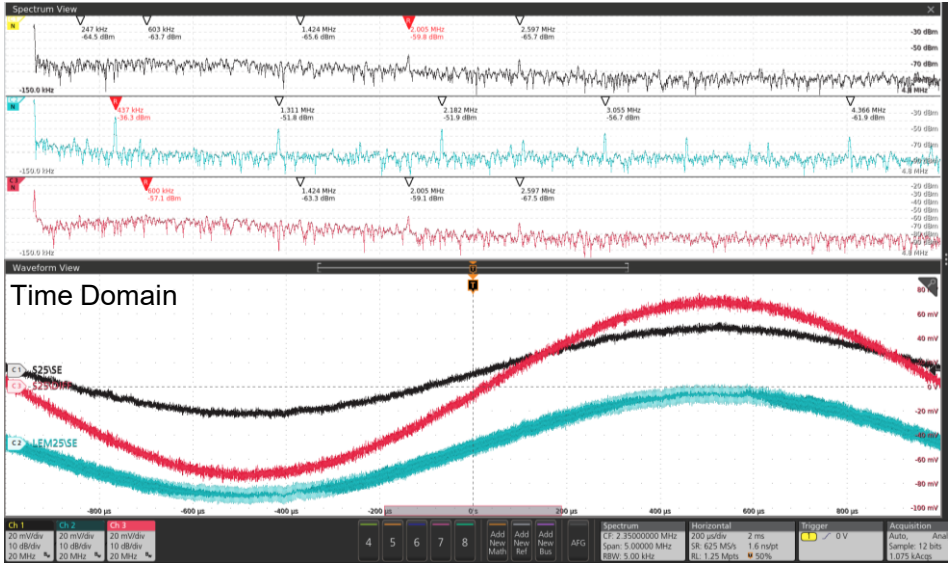

Experimental Evaluation 3

AC Impedance Measurement: Methodology

- Purpose: Evaluate dynamic impedance of sensor output stage across frequency sweep (100 Hz – 10 Mhz)
- Equipment: Bode 100 VNA, APS 1000 amplifier, probes
- Input: 1.175 A_{RMS} sinusoidal current
- Impedance calculated via CH1 (current), CH2 (voltage):

$$Z(f) = \frac{V_{\text{out}}(f)}{I_{\text{in}}(f)} = \frac{V_{\text{CH2}}(f)}{V_{\text{CH1}}(f)}$$

- Measurement limit: Reliable up to **~50 kHz** due to APS 1000 amplifier output drop-off

Test Setup [29]

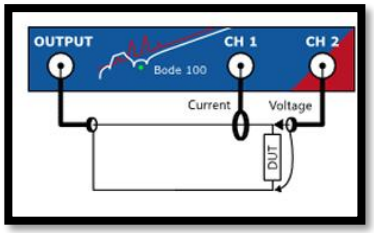

Test setup

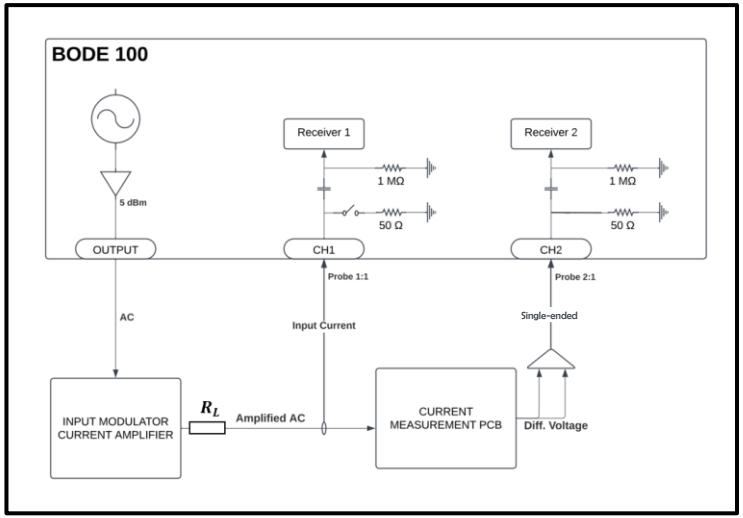

Experimental Evaluation 3

AC Impedance Measurement: Results

- Initial impedance (at 100 Hz) aligns with G_{meas}, measured in DC test ($G_{err} = 0.82\ \%$ and $G_{err} = 1.25\ \%$).
- Overall flat and stable impedance response for both sensors
- Slightly flatter magnitude and phase response for **Closed-loop Fluxgate**
- The phase response remains flat below 20 kHz and gradually drops approaching 50 kHz.
- Distinct rise near 2 kHz in **Closed-loop TMR** sensor:

  → due to internal operating transition (field-sensor-controlled operation to transformer-like behavior)

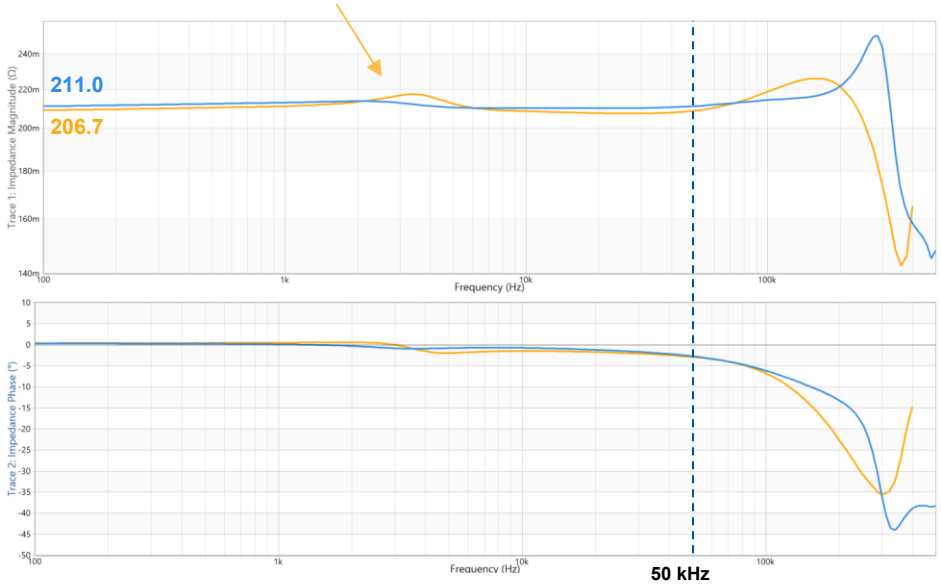

Fig. 7: Bode diagram showing impedance magnitude and phase response of tested sensors under a sinusoidal current input of 1.175 A_{RMS}.

Summary

Research Internship

- Designed and validated a differential analog current measurement PCB for isolated three-phase sensing
- Integrated within UltraZohm system and ADC interface
- Developed a AC + DC test setup
- Performed full characterization of closed-loop TMR and Fluxgate sensors

Seminar

- Evaluated DC accuracy, time- and frequency response and dynamic behavior of multiple magnetic field-based sensor types (Hall-effect, open-loop AMR, open-loop TMR, closed-loop TMR).

Chair of High-Power Converter Systems
TUM School of Engineering and Design
Technical University of Munich

A Comparative Study of Magnetic Current Sensor Technologies with Experimental Evaluation Across Time, Frequency and Impedance Domains

Kaan Ilhan

Technische Universität München

Chair of High-Power Converter Systems

25. July 2025

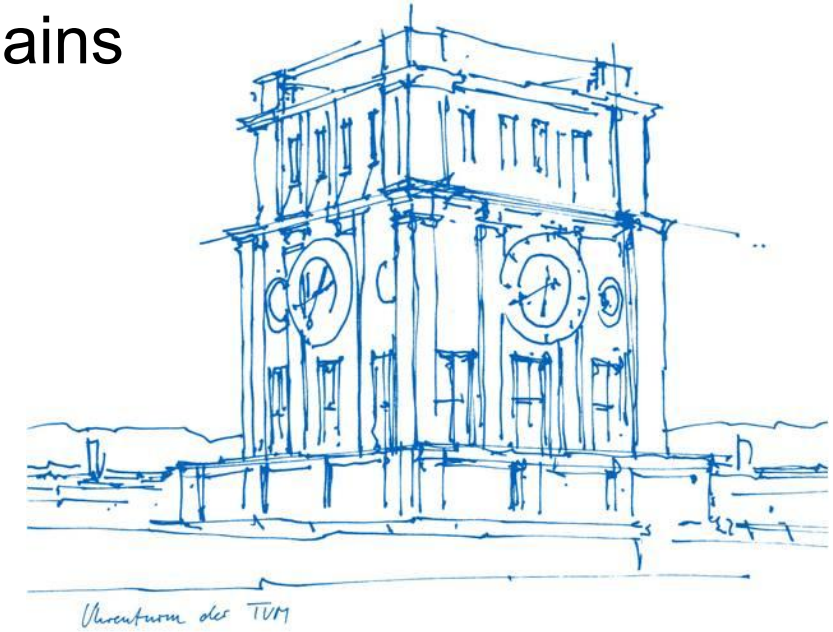

Current Measurement PCB – Rev2

- 4-layer PCB for analog current measurements with 4 channels
- Up to 130 A DC continuous current
- Supports sensors with THD-10 footprint (Sensitec CAS5000, LEM CASR etc.)
- Compatible with UltraZohm platform (RJ45 differential output)
- V_{OCM}= 2.5 V
- Thermal safe limit: 100 °C at 120 A (tested)
- Phase-to-phase clearance/creepage: 9 mm/10mm

  → Maximum phase-to-phase: 1000 V_{RMS} (compliant with IEC 60664-1)
- Redesigned power supply with integrated buck module:

  → reduced EMI resulting from 300 kHz switching noise;

  → output current increased to 1 A based on sensor load

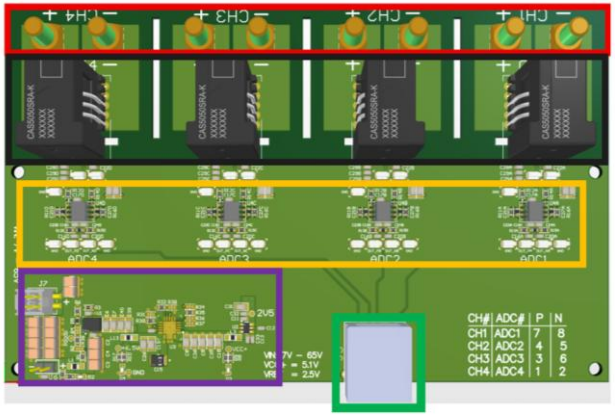

Fig. 4: 3D layout view of the custom 4-layer current measurement PCB with color highlighted key blocks: Current input terminals (red), Sensitec sensors (black), differential amplifiers (yellow), power supply circuitry (purple) and Ethernet signal outputs (green).

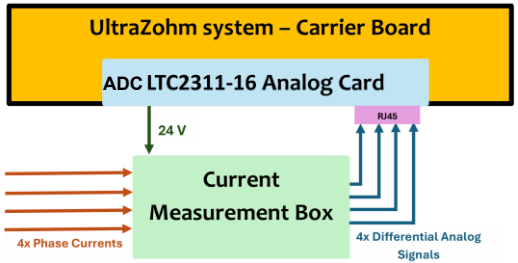

– Rev 1 –

Sinusoidal current input: 1 A_{RMS} @ 500 Hz

LEM CASR 6
(Fluxgate)

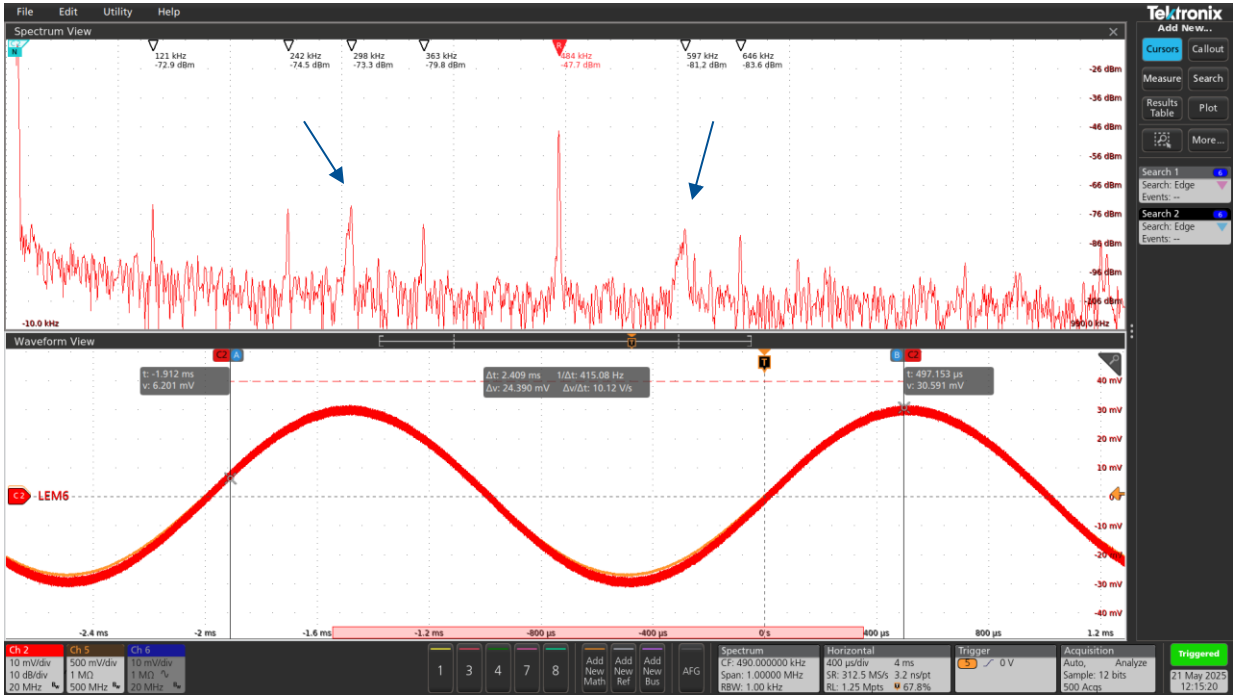

Current Measurement PCB

– Rev1 –

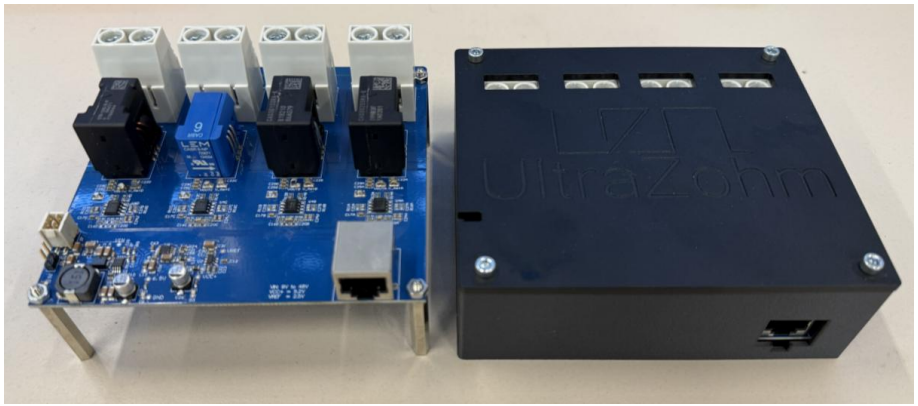

– Rev2 –

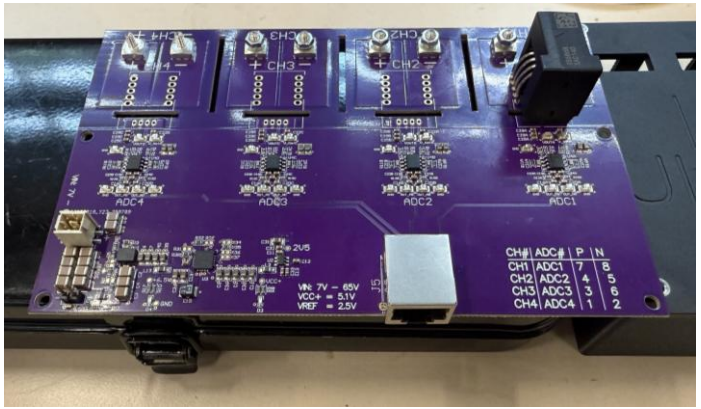

Sensor Portfolio

- Purpose: to evaluate their performance and compare the actual performance vs datasheet.

  1) DC output characterization

  2) Time- and frequency domain observation

  3) AC impedance measurement.

With Evaluation Board

With Custom PCB (Rev 2)

	Datasheet			
Sensor	I_{nom} (A)	f_{BW} (Hz)	I_{ND} ($\mu A/\sqrt{Hz}$)	$G_{theoretical}$ (mV/A)
Open-Loop Hall-Effect Sensors (Allegro). Package: SOICW-16				
ACS37002LMABTR-050B5-M	±50	400k	350	40.0
ACS37002LMCATR-090B5	±90	400k	350	22.2
Open-Loop AMR Sensors (Aceinna). Package: SOICW-16				
MCA1101-5-5	±5	1.5M	10	350.0
MCA1101-20-5	±20	1.5M	10	90.0
MCA1101-50-5	±50	1.5M	10	35.0
Open-Loop TMR Sensor (Allegro). Package: SOICW-16				
CT432-HSWF50MR	±50	1M	44.3	40.0
Closed-Loop TMR Sensors (Sensitec). Package: THD-8 (KH)				
CAS5050SRA-KH	±50	400k	N/A	12.5
CAS5075KRA-KH	±75	400k	N/A	6.25

Experimental Evaluation 1

DC Measurement: Methodology & Metrics

- DC sweep to measure sensors' linear voltage response
- Metrics: **Gain error**, **Linearity error**, **Offset error**
- Reference: Manufacturer datasheet vs. measured output

$$V_{out} = G \cdot I_{in} + b$$

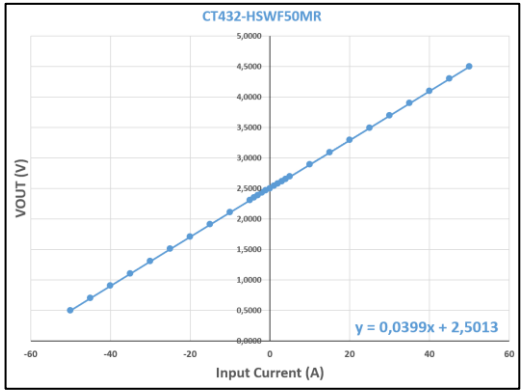

$$\varepsilon_{acc} = \underbrace{\left|\frac{G_{measured} - G_{theoretical}}{G_{theoretical}}\right| \times 100\%}_{\text{Gain error}} + \underbrace{|r|}_{\text{Linearity error}} + \underbrace{\left|\frac{b - V_{ref}}{y_{FS}}\right| \times 100\%}_{\text{Offset error}}$$

$$r = \pm\frac{\Delta L_{max}}{y_{FS}} \times 100\%$$

$$y_{FS} = G_{meas} \cdot I_N$$

	Datasheet			Measured/Calculated				
Sensor	f_{BW} (Hz)	I_{ND} ($\mu A/\sqrt{Hz}$)	$G_{theoretical}$ (mV/A)	$G_{measured}$ (mV/A)	b (V)	ΔL_{max} (mV)	r (%)	ε_{acc} (%)
Open-Loop Hall-Effect Sensors (Allegro). Package: SOICW-16								
ACS37002LMABTR-050B5-M	400k	350	40.0	36.1	2.502	8.3 @ −35 A	0.23	11.63
ACS37002LMCATR-090B5	400k	350	22.2	21.7	2.4999	5.4 @ −3 A	0.138	3.08
Open-Loop AMR Sensors (Aceinna). Package: SOICW-16								
MCA1101-5-5	1.5M	10	350.0	333.4	2.1983	−91.0 @ −4 A	−2.73	7.50
MCA1101-20-5	1.5M	10	90.0	89.6	2.1796	−13.6 @ −2 A	−0.38	1.06
MCA1101-50-5	1.5M	10	35.0	34.7	2.1777	42.7 @ 50 A	1.23	2.37
Open-Loop TMR Sensor (Allegro). Package: SOICW-16								
CT432-HSWF50MR	1M	44.3	40.0	39.9	2.501	7.9 @ 4 A	0.198	0.52
Closed-Loop TMR Sensors (Sensitec). Package: THD-8 (KH)								
CAS5050SRA-KH	400k	N/A	12.5	12.5	2.4933	−1.7 @ 50 A	−0.136	0.32
CAS5075KRA-KH	400k	N/A	6.25	6.22	2.501	−1.7 @ 75 A	−0.182	0.35

Experimental Evaluation 1

DC Measurement: Results

$$\varepsilon_{\text{acc}} = \underbrace{\left|\frac{G_{\text{measured}} - G_{\text{theoretical}}}{G_{\text{theoretical}}}\right| \times 100\%}_{\text{Gain error}} + \underbrace{|r|}_{\text{Linearity error}} + \underbrace{\left|\frac{b - V_{\text{ref}}}{y_{\text{FS}}}\right| \times 100\%}_{\text{Offset error}}$$

- Closed-loop TMR sensors: best accuracy (ε_{acc} < 0.35%)
- Open-loop Hall sensors: highest error (ε_{acc} up to 11%)
- AMR sensors: good gain, but gain & linearity issues in lower range variant
- Open-loop TMR: excellent overall accuracy (ε_{acc} ~0.5%) despite simplicity
- Closed-loop + MR technology = best trade-off in precision & stability

	Datasheet			Measured/Calculated				
Sensor	f_{BW} (Hz)	I_{ND} (μA/$\sqrt{\text{Hz}}$)	$G_{\text{theoretical}}$ (mV/A)	G_{measured} (mV/A)	b (V)	$\Delta L_{\max}$ (mV)	r (%)	ε_{acc} (%)
Open-Loop Hall-Effect Sensors (Allegro). Package: SOICW-16								
ACS37002LMABTR-050B5-M	400k	350	40.0	36.1	2.502	8.3 @ −35 A	0.23	11.63
ACS37002LMCATR-090B5	400k	350	22.2	21.7	2.4999	5.4 @ −3 A	0.138	3.08
Open-Loop AMR Sensors (Aceinna). Package: SOICW-16								
MCA1101-5-5	1.5M	10	350.0	333.4	2.1983	−91.0 @ −4 A	−2.73	7.50
MCA1101-20-5	1.5M	10	90.0	89.6	2.1796	−13.6 @ −2 A	−0.38	1.06
MCA1101-50-5	1.5M	10	35.0	34.7	2.1777	42.7 @ 50 A	1.23	2.37
Open-Loop TMR Sensor (Allegro). Package: SOICW-16								
CT432-HSWF50MR	1M	44.3	40.0	39.9	2.501	7.9 @ 4 A	0.198	0.52
Closed-Loop TMR Sensors (Sensitec). Package: THD-8 (KH)								
CAS5050SRA-KH	400k	N/A	12.5	12.5	2.4933	−1.7 @ 50 A	−0.136	0.32
CAS5075KRA-KH	400k	N/A	6.25	6.22	2.501	−1.7 @ 75 A	−0.182	0.35

Experimental Evaluation 2

Time & Frequency Domain Observations: Methodology

- Sinusoidal current input: 0.5 A_{RMS} @ 1 kHz
- Single ended probes for sensor voltage outputs
- Each output waveform is normalized by Gain → **normalized current-equivalent outputs**
- FFT analysis identifies: Internal modulation tones (spikes), noise floor (broadband interference), spectral content…
- Sensor bandwidth impacts:
    a. ripple suppression ability
    b. Signal fidelity
    c. Passing through more high-frequency noise

Experimental Evaluation 2

Time & Frequency Domain Observations

- **Open-loop AMR** & **Open-loop TMR:** Best signal clarity lowest ripple, flattest FFT noise. Minimal spectral content.
- **Closed-loop TMR (50A)**: moderate ripple; slightly elevated noise floor. Low broadband noise
- **Closed-loop TMR (75A)**: highest ripple due to elevated noise floor
- **Hall-Effect:** Both with high ripple due to elevated noise floor and dominant internal modulation spike at ~973 kHz

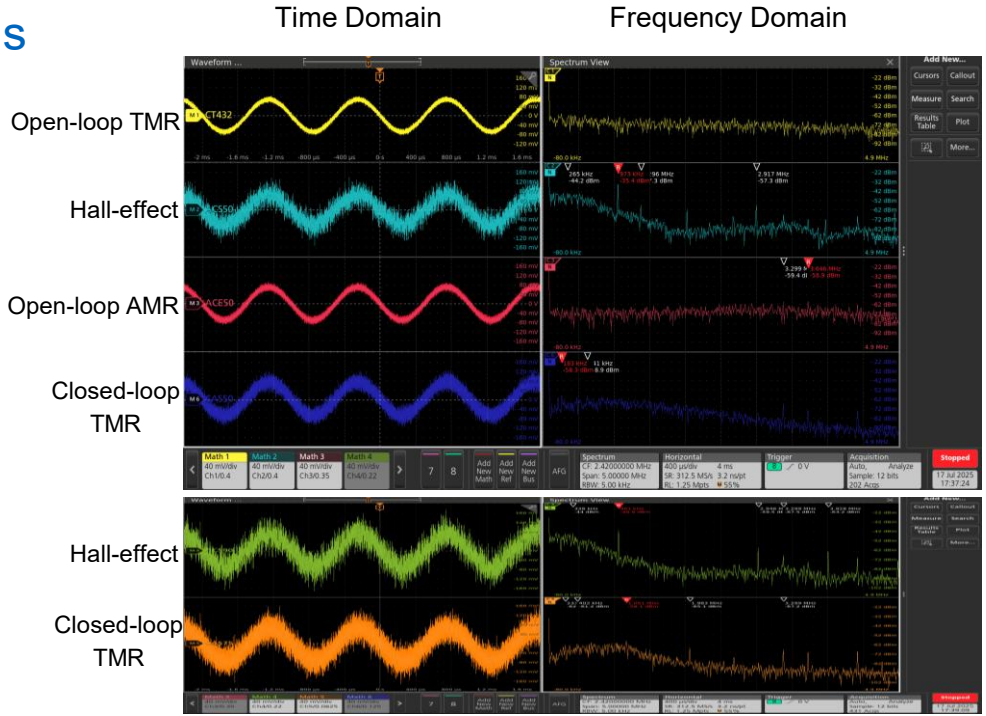

→ FFT vs. datasheet noise: no direct correlation!
Lowest noise density (I_{ND}) sensors did not necessarily show better performance

Experimental Evaluation 3

AC Impedance Measurement: Methodology

- Purpose: Evaluate dynamic impedance of sensor output stage across frequency sweep (10 Hz – 10 Mhz)
- Equipment: Bode 100 VNA, APS 1000 amplifier, probes
- Input: 1.175 A_{RMS} sinusoidal current
- Impedance calculated via CH1 (current), CH2 (voltage):

$$Z(f) = \frac{V_{\text{out}}(f)}{I_{\text{in}}(f)} = \frac{V_{\text{CH2}}(f)}{V_{\text{CH1}}(f)}$$

- Measurement limit: Reliable up to **~50 kHz** due to APS 1000 amplifier output drop-off

Test Setup [29]

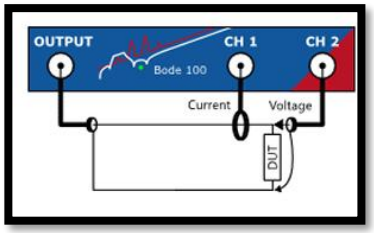

Test setup

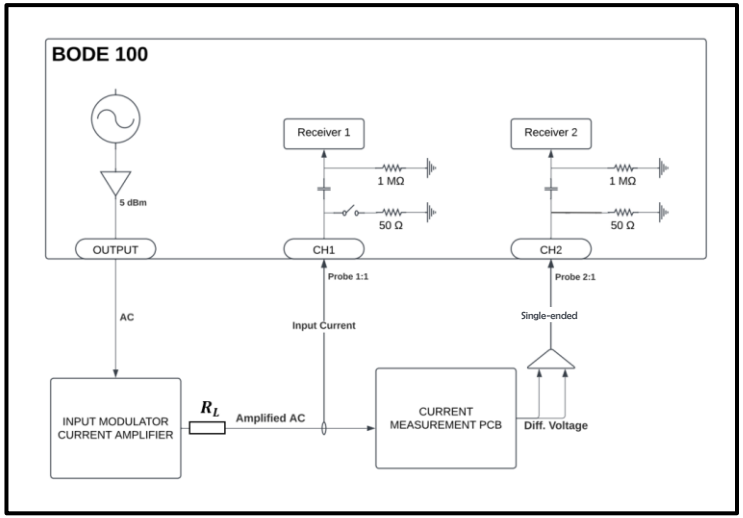

Experimental Evaluation 3

AC Impedance Measurement: Results

- Initial impedance (at 10 Hz) aligns with G_{meas}, measured in DC test.
- Flat and stable impedance response for **Open-loop TMR** and **Open-loop AMR** sensors
- Sharp zigzag fluctuations for **Hall-Effect** sensors: indicates internal frequency-dependent Gain changes.
- Distinct dip near 2 kHz for both **Closed-loop TMR** sensors:

→ due to internal operating transition (field-sensor-controlled operation to transformer-like behavior)

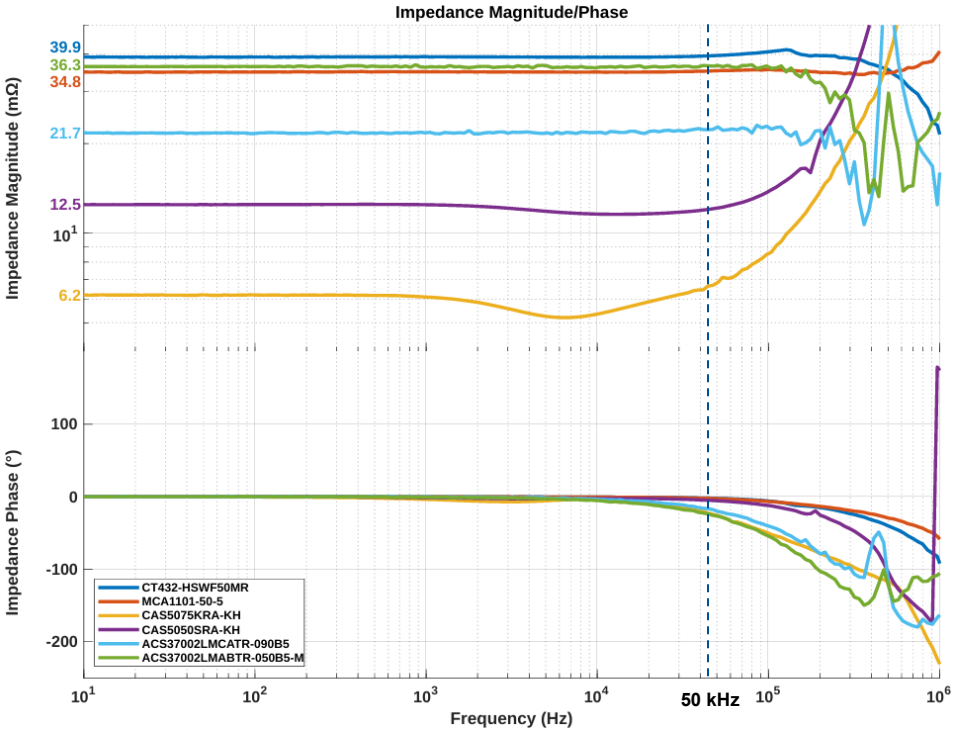

Fig. 7: Bode diagram showing impedance magnitude and phase response of tested sensors under a sinusoidal current input of 1.175 A_{RMS}.

Conclusion

- Hall-effect sensors:
  - → Poor gain precision
  - → High thermal drift under static load
  - → High broadband noise + modulation tones → High ripple
- AMR & open-loop TMR sensors:
  - → Lowest noise, flat FFT → minimal ripple
- AC impedance:
  - → AMR & TMR = most stable dynamic behavior
- **Variants matter:**
  - → Closed-loop TMR models from same brand (Sensitec) showed different results
- AMR & TMR suitable for high-current, fast-switching inverters (e.g. SiC inverters)

References

[1] P. Niklaus, D. Bortis, and J. W. Kolar, “High-Bandwidth High-CMRR Current Measurement for a 4.8 MHz Multi-Level GaN Inverter AC Power Source,” APEC, 2021.
[2] Allegro Microsystems, “From Hall Effect to TMR: A Comparison of Magnetic Sensing Technologies,” AN117, 2023.
[3] Allegro Microsystems, “Achieving Closed-Loop Accuracy in Open-Loop Current Sensors,” 2023.
[4] B. Mammano, Current Sensing Solutions for Power Supply Designers, TI Seminar SEM1200, SLUP114, 1997.
[5] H. Kirkham, “Current Measurement Methods for the Smart Grid,” IEEE Power Engineering Society General Meeting, 2009.
[6] S. C. Mukhopadhyay and R. Y. M. Huang, Sensors, Springer, 2008, pp. 23–43.
[7] H. Deng et al., “High Precision Closed-loop TMR Current Sensor for Small Current Measurement,” IAECST, 2023.
[8] Allegro Microsystems, CT432: XtremeSense TMR Current Sensor, Rev. 2, Nov. 2023.
[9] Allegro Microsystems, ACS37002: Hall Effect Current Sensor IC, Rev. 1.0, 2021.
[10] Allegro Microsystems, ACSEVB-MC16 Evaluation Board User Guide, Aug. 2023.
[11] ACEINNA Inc., MCx1101 EVB User Manual, v1.3, 2021. Available: aceinna.com
[12] ACEINNA, MCA1101-xx-5 Datasheet, Rev. L, June 2024.
[13] Sensitec GmbH, CAS5000-Series Datasheet, Rev. 02/2022.
[14] Würth Elektronik eiSos GmbH, 7461001 Terminal Datasheet, v3.0, June 2023.
[15] Texas Instruments, THS4521 Amplifier Datasheet, Rev. G, July 2023.
[16] Texas Instruments, REF35250 Voltage Reference, Rev. D, Oct. 2023.
[17] Texas Instruments, TPSM365R3 Power Module, Rev. A, June 2024.
[18] Texas Instruments, TPS7A47 LDO Regulator, Rev. I, Apr. 2023.
[19] IEC 60664-1, Insulation Coordination for Equipment, May 2020.
[20] IEC 61800-5-1, Adjustable Speed Drive Systems Safety, Aug. 2022.
[21] IPC-9592B, Power Conversion Device Requirements, Jan. 2013.
[22] IPC-2221B, Standard on PCB Design, Nov. 2012.
[23] W. Zhang and T. LaBella, “Demystifying Clearance and Creepage,” TI Power Supply Design Seminar, SLUP419, 2024.
[24] M. Lei et al., “TMR Sensor with Temperature Compensation,” Energy Reports, vol. 8, pp. 137–146, 2022.
[25] M. Cerna and A. F. Harvey, “Fundamentals of FFT-Based Signal Analysis,” NI App Note 041, 2000.
[26] Spitzenberger & Spies, APS 1000 Amplifier Overview, Rev. 1107-e-0008-1.
[27] B. Zhang, “Time-delay Compensation Techniques,” PEMC Conference, 2015.
[28] Anup Bhalla, “Practical considerations when comparing SiC and GaN in power applications,” *Elettronica-Plus*, July 17, 2018. [Online]. Available: https://elettronica-plus.it/practical-considerations-when-comparing-sic-and-gan-in-power-applications_96479/. [Accessed: Jul. 22, 2025].
[29] OMICRON Lab, *Bode Analyzer Suite - User Manual*, Rev. 3.5. OMICRON electronics GmbH, Austria, 2022. [Online]. Available: https://www.omicron-lab.com/fileadmin/assets/Bode-Analyzer-Suite/Documents/Bode-Analyzer-User-Manual.pdf. [Accessed: Jul. 22, 2025].